

# **Radiative Impacts of Anvil Outflow During the Maritime Continent Thunderstorm Experiment**

*M. P. Jensen and T. P. Ackerman  
Department of Meteorology  
Pennsylvania State University  
University Park, Pennsylvania*

*S. M. Sekelsky  
Department of Electrical Engineering  
University of Massachusetts  
Amherst, Massachusetts*

## **Introduction**

The Maritime Continent Thunderstorm Experiment (MCTEX) took place from November 13 to December 10, 1995, on the Tiwi Islands, Australia (Figure 1). The primary objective of the field experiment was to study the life cycles of the thunderstorms, which occur almost daily on these islands during the transition between wet and dry seasons. As part of this experiment, a suite of remote sensing instruments including a dual wavelength millimeter radar consisting of 3-mm (W-band) and 9-mm (Ka-band) subsystems, a 10-cm (S-band) vertically pointing radar, a Microwave Radiometer, a lidar, and broadband solar and infrared (IR) radiometers were deployed at the village of Garden Point on Melville Island (11.4S, 130.41E). Soundings were acquired at Maxwell Creek (11.55S, 130.56E) and a 5-cm scanning Doppler radar was operated at Nguui (10.23S, 130.62E) on Bathhurst Island.

## **Case Study**

On November 27, 1995, convection developed over Apsley Strait at about 0330 Universal Time Coordinates (UTC) (1330 LT). This area has been shown to be a preferential area for development over the Tiwi Islands (Keenan et al. 1990). This convective cell drifted towards the west leaving a trailing cirrus anvil. The cirrus spread north/south arriving over the Garden Point site at about 0530 UTC at a height of 12 km to 15 km. A few hours later (0730 UTC), the radar shows a lower but thicker cirrus layer at the Garden Point site extending from 6 km to 13 km and lasting until 1030 UTC. As the cirrus anvil moved over the Garden Point site, the downward solar irradiance dropped from 900 W/m<sup>2</sup> to about 150 W/m<sup>2</sup> (0530 UTC) suggesting that even the edges of the anvil have large optical depths.



**Figure 1.** The Tiwi Islands showing locations of MCTEX surface remote sensing sites (<http://www.atmos.washington.edu/gcg/Mctex.site/>).

## Microphysical Calculations

The presence of radar observations at several different wavelengths permitted the analysis of some of the microphysical properties of cirrus anvils. Sekelsky et al. (1999) use a radar dual-wavelength technique in order to determine some of the microphysical properties of the cloud. The dual wavelength ratio (DWR) is given by  $DWR_{l,h} = 10 \log(Z_{e,l}/Z_{e,h})$  where the l denotes the lower frequency radar band and the h denotes the higher frequency radar band. If we make the assumption that the ice cloud particles follow a first-order gamma distribution given by  $N(D) = N_0 D \exp^{-4.67D/D_0}$ , the DWR depends only on the median radius,  $D_0$ , and to a lesser degree on the density,  $\rho$  (Sekelsky et al. 1999).

This retrieval was done by Sekelsky et al. (1999) for a period of about an hour for three separate cases representing a thin cirrus case near the edge of the anvil (November 27), a thicker stratiform case (November 28), and a convective region case (December 4). The result is a time-height profile of median size and number density for each case. Integrating the first-order gamma distribution for all diameters we can determine the total volume density of particles in each radar volume, and multiplying by the appropriate density function we can determine the time-height profile of ice water content (IWC).

Using the S-band reflectivities along with the IWC determined from Sekelsky et al.'s (1999) retrieval, a Z-IWC parameterization appropriate for each case was chosen. For the cirrus regime (November 27)  $IWC = 0.55Z_i^{0.36}$ . For the stratiform regime (November 28)  $IWC = 0.01Z_i^{0.84}$  and for the convective regime  $IWC = 2.5 \text{ g/kg}$ . Each one of these cases is then taken to be representative of a region of a typical island thunderstorm.

In addition to the three vertically pointing radars at the Garden Point site, there was a scanning C-band (5.3 cm) radar located in the township of Nguiu on the southeast corner of Bathurst Island. This radar with its scanning capabilities allows three-dimensional (3-D) sampling of the cloud structure as it evolves in time. Previous work (Keenan et al. 1990, 1994) has investigated the development and structure of the island-generated thunderstorms over the Tiwi Islands, but with an emphasis on the convective core and dynamics of the system. Here we emphasize the development and extent of the anvil outflow with the goal of describing the radiative impacts of these systems. Figure 2 shows horizontal cross sections of C-band radar reflectivity at a height of 8 km for six different stages in the development of the cirrus outflow for the November 27 case. Figure 2a shows a band of strong echoes oriented east-west. This development pattern has been previously noted by Keenan et al. (1990, 1994) and attributed to the development of storms along sea-breeze convergence lines. There is no discernible anvil at this time. Approximately an hour and a half later (Figure 2b), the weak cells have merged into a more substantial mesoscale system. Reflectivities are as high as 45 dBZe in the core of the updraft and we see the initial formation of an anvil at upper levels. A half hour later (Figure 2c), there is an extension of a horizontally constrained deep anvil layer. This layer extends from about 5 km to about 14 km, and has a width approximately equal to the width of the convective updraft with average reflectivities on the order of 20 dBZe. After another hour (Figure 2d), the system cloud shield now covers an area of approximately 6000 km<sup>2</sup>. The convective core has moved from over Apsley Strait to approximately 40 km west of Bathurst Island. During this stage there is a spreading of the anvil at upper levels in the north-south direction, while at lower levels it does not change width very much. As the anvil spreads out, the ice crystals start settling and we see the anvil layer start to fall, such that at 0734 UTC (Figure 2e) the reflectivity at 14 km is already much lower. Later, the region of highest reflectivities moves lower, until the final stage in the life cycle of the storm (Figure 2f), where the remnant of the anvil is a cirriform layer between about 5 km and 8 km.

Comparison of C-band reflectivities with W-, Ka-, and S-band reflectivities makes it possible to apply some of the microphysical information over a larger area. After checking that the S- and C-band reflectivities were in general agreement over the Garden Point site, we apply these parameterizations to the C-band reflectivities. In order to apply these parameterizations, it must be realized that the particle size distributions change as a function of time and space during the evolution of the cloud system. In order to begin to address this difficulty, we have divided the cloud system into three separate regimes by reflectivity criteria, corresponding to the three different regimes observed in the three case studies. We therefore apply the cirrus parameterization for  $-8 < \text{dBZe} < 7$ , the stratiform parameterization for  $7 < \text{dBZe} < 23$ , and the convective parameterization when  $\text{dBZe} < 23$ .

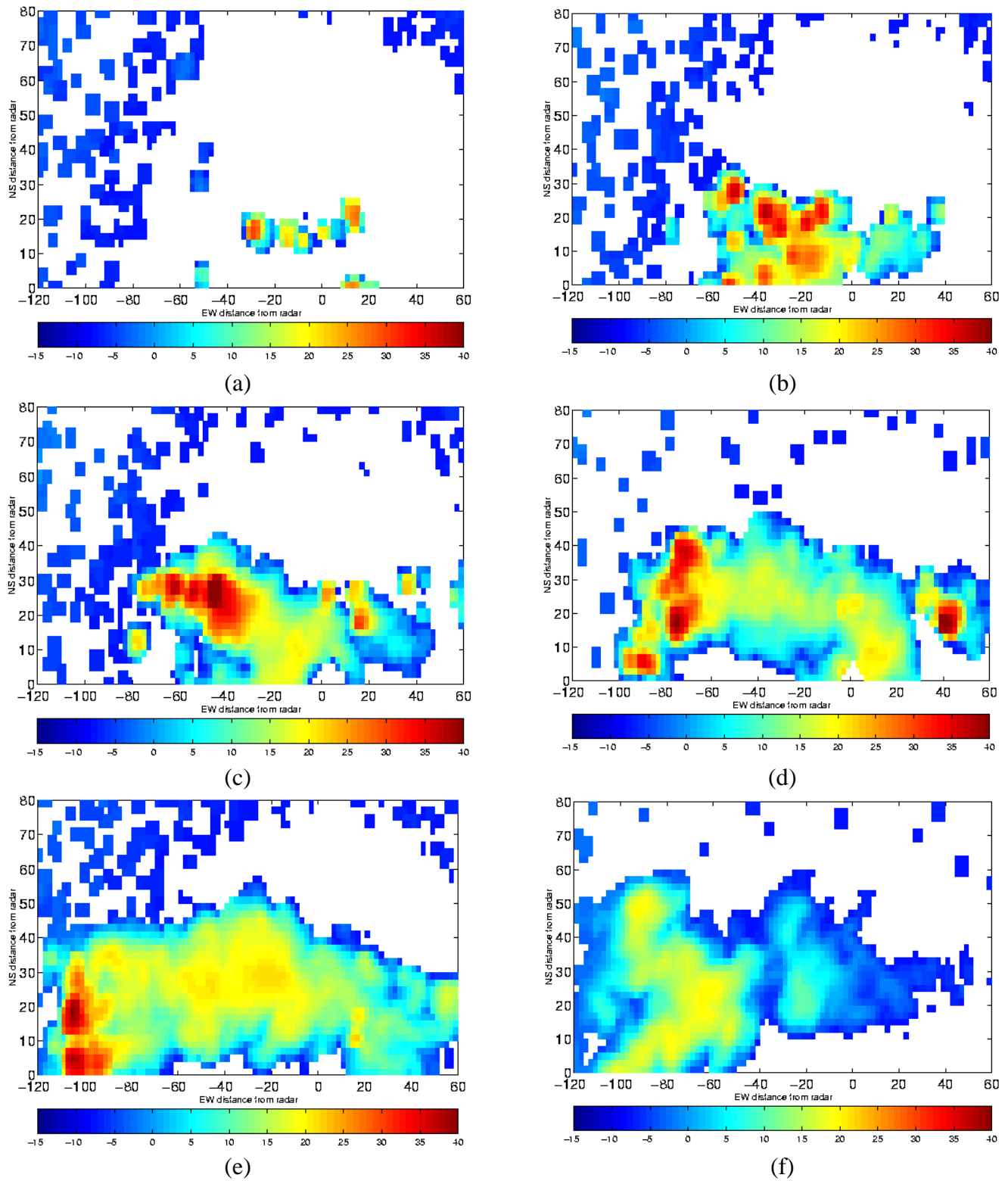


**Figure 2.** C-band radar reflectivities at a height of 8 km at a) 0334 UTC, b) 0502 UTC, c) 0537 UTC, d) 0633 UTC, e) 0734 UTC, and f) 0935 UTC.

## **Heating Rates**

The RAPid RADiative transfer model (RAPRAD) (Toon et al. 1989) is used to calculate broadband fluxes through the cloud layer. This model uses a two-stream approximation for scattering and a correlated-k technique for absorption for 26 bands in the solar spectrum from 0.25 microns to 4.5 microns and 18 bands in the IR. Gaseous absorption by H<sub>2</sub>O, CO<sub>2</sub>, and O<sub>3</sub> is included. The profiles of temperature and water vapor used in the calculations are taken from a nearby sounding just before the initiation of convection. We consider a volume over the Tiwi Islands with dimensions 80 km x 180 km x 20 km. This volume is divided into columns with dimensions 2 km x 2 km x 20 km. An independent pixel approximation is used for the radiative transfer calculations (i.e., we treat each column individually as plane-parallel and homogeneous in each of 11 layers neglecting interactions between columns. A cloudy layer is defined by a log-normal distribution of cloud particles). We assume a constant value for the standard deviation of the distribution of 1.62. The mean particle radius is assumed to remain constant within each of the three regimes;  $r = 50$  microns (cirrus case),  $r = 250$  microns (stratiform case) and  $r = 425$  microns (convective case). Finally, the cloud particle number density is backed out from the IWC calculated from the C-band radar reflectivity using the Z-IWC parameterizations discussed above. This analysis results in a 3-D representation of the radiative transfer through the anvil system at six different stages of the anvil life cycle.

In order to compare these heating rates, previous studies, the heating rate profiles are averaged over all profiles within the anvil region of the cloud. These results are compared to a modeling study of the radiative properties of oceanic thunderstorms in the maritime continent region (Wong et al. 1993). Figure 3 shows that the island-generated thunderstorms have peak solar heating (IR cooling) at higher heights in the atmosphere compared to their oceanic counterparts. This is presumably due to ice being transported higher in the atmosphere by the island-generated thunderstorms by stronger updrafts enhanced by land-sea contrasts. The magnitude of this heating is also a great deal more in the island thunderstorms compared the oceanic storms. It is important to note that in Figure 3 the radiative properties below cloud base are not taken into account; this should not affect our results of cloud top radiative processes because of the large optical depths of the cloud layer.

## **Acknowledgments**

This work was supported by Pacific Northwest National Laboratory, Subcontract No. 091572-A-Q1 under U.S. Department of Energy Prime DE-AC06-76RLO 1830. We would also like to thank Tom Keenan and Michael Whimply from the Bureau of Meteorological Research Center (BMRC) for their help with the C-band radar and satellite data, Warner Ecklund from the National Oceanic and Atmospheric Administration (NOAA) for his help with the S-band radar data, and Johannes Verlinde from Pennsylvania State University (PSU) for his help with the radar data processing.

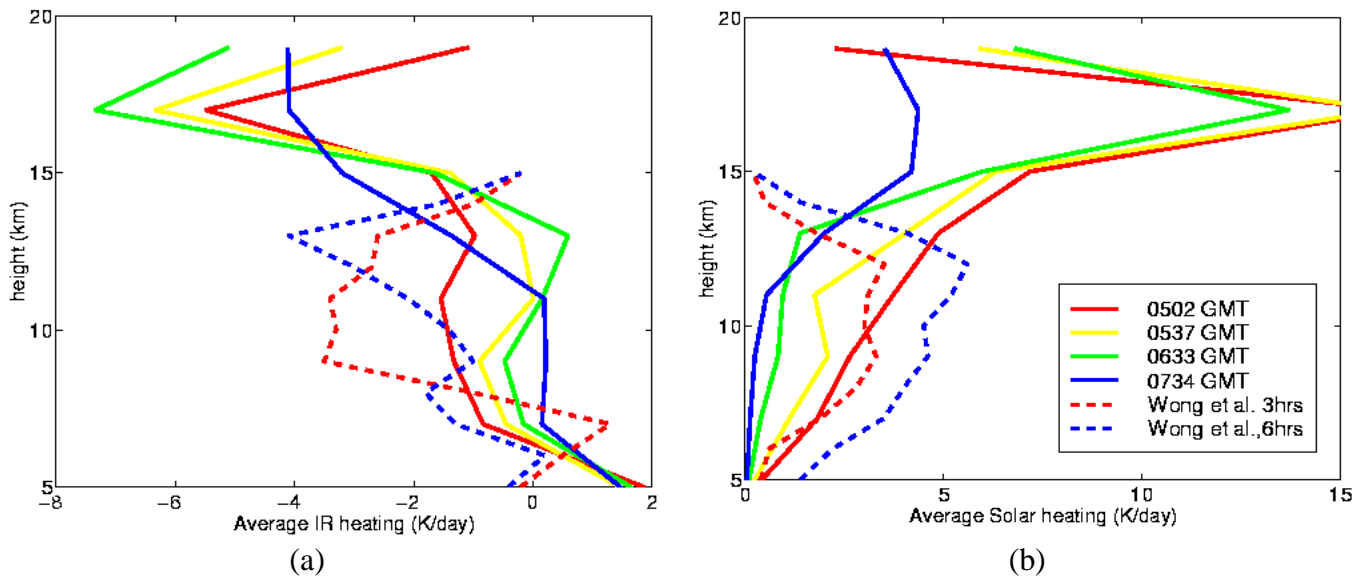


**Figure 3.** Average heating rate profiles: (a) IR, (b) solar for four different stages of the anvil life cycle compared to modeling results from Wong et al. (1993).

## References

Keenan, T. D., B. Ferrier, and J. Simpson, 1994: Development and structure of a maritime continent thunderstorm. *Meteor. Atmos. Phys.*, **53**, 185-222.

Keenan, T. D., B. R. Morton, X. S. Zhang, and K. Nyguen, 1990: Some characteristics of thunderstorms over Bathurst and Melville Islands near Darwin, Australia. *Quart. J. Roy. Met. Soc.*, **116**, 1153-1172.

Sekelsky, S. M., W. L. Ecklund, J. M. Firda, K. S. Gage, and R. E. McIntosh, 1999: Particle size estimation in ice-phase clouds using radar reflectivity measurements collected at 95 GHz, 33 GHz and 2.8 GHz. *J. Appl. Meteo.* Accepted for publication.

Toon, O. B., C. P. McKay, T. P. Ackerman, and K. Santhanam, 1989: Rapid calculation of radiative heating rates and photodissociation rates in inhomogeneous multiple scattering atmospheres. *J. Geophys. Res.*, 16,287-16,301.

Wong, T., G. L. Stephens, and P. W. Stackhouse, 1993: The radiative budgets of a tropical mesoscale convective system during the EMEX-STEP-AMEX Experiment. 1. Model Results. *J. Geophys. Res.*, 8695-8711.